2-12-2015

Abnormal myofiber morphology and limb dysfunction in claudication

Panagiotis Koutakis
University of Nebraska at Omaha

Sara A. Myers
University of Nebraska at Omaha, samyers@unomaha.edu

Kim Cluff

Duy M. Ha

Gleb Haynatzki

See next page for additional authors

Recommended Citation

Koutakis, P, Myers, SA, Cluff, K, Ha, D, Haynatzki, G, McComb, R, Uchida, K, Miserlis, D, Papoutsi, E, Johanning, J, Casale, G, Pipinos, I. Abnormal myofiber morphology and limb dysfunction in claudication. Journal of Surgical Research. 2015; Jun 1; 196(1):172-9. PMCID: PMC4512658. https://doi.org/10.1016/j.jss.2015.02.011

Abnormal myofiber morphology and limb dysfunction in claudication

Panagiotis Koutakis, MS,[a] Sara A. Myers, PhD,[b] Kim Cluff, PhD,[c] Duy M. Ha, BS,[a] Gleb Haynatzki, PhD,[d] Rodney D. McComb, MD,[e] Koji Uchida, PhD,[f] Dimitrios Miserlis, MD, BS,[a] Evlampia Papoutsi, BS,[a] Jason M. Johanning, MD,[a,g] George P. Casale, PhD,[a], and Iraklis I. Pipinos, MD, PhD[a,g]

a Department of Surgery, University of Nebraska Medical Center, Omaha, Nebraska
b Nebraska Biomechanics Core Facility, University of Nebraska Omaha, Omaha, Nebraska
c Department of Industrial & Manufacturing Engineering, Wichita State University, Wichita, Kansas
d Department of Biostatistics, College of Public Health, University of Nebraska Medical Center, Omaha, Nebraska
e Department of Pathology and Microbiology, University of Nebraska Medical Center, Omaha, Nebraska
f Laboratory of Food and Biodynamics, Graduate School of Bioagricultural Sciences, Nagoya University, Nagoya, Japan
g Department of Surgery and VA Research Service, VA Nebraska-Western Iowa Health Care System, Omaha, Nebraska

Keywords:

Claudication, Walking distance, Myofiber morphology

ABSTRACT

Background: Peripheral artery disease (PAD), which affects an estimated 27 million people in Europe and North America, is caused by atherosclerotic plaques that limit blood flow to the legs. Chronic, repeated ischemia in the lower leg muscles of PAD patients is associated with loss of normal myofiber morphology and myofiber degradation. In this study, we tested the hypothesis that myofiber morphometrics of PAD calf muscle are significantly different from normal calf muscle and correlate with reduced calf muscle strength and walking performance.

Methods: Gastrocnemius biopsies were collected from 154 PAD patients (Fontaine stage II) and 85 control subjects. Morphometric parameters of gastrocnemius fibers were determined and evaluated for associations with walking distances and calf muscle strength.

Results: Compared with control myofibers, PAD myofiber cross-sectional area, major and minor axes, equivalent diameter, perimeter, solidity, and density were significantly decreased ($P < 0.005$), whereas roundness was significantly increased ($P < 0.005$). Myofiber morphometric parameters correlated with walking distances and calf muscle strength. Multiple regression analyses demonstrated myofiber cross-sectional area, roundness, and solidity as the best predictors of calf muscle strength and 6-min walking distance, whereas cross-sectional area was the main predictor of maximum walking distance.

Conclusions: Myofiber morphometrics of PAD gastrocnemius differ significantly from those of control muscle and predict calf muscle strength and walking distances of the PAD patients. Morphometric parameters of gastrocnemius myofibers may serve as objective criteria for diagnosis, staging, and treatment of PAD.

1. Introduction

Peripheral artery disease (PAD) affects an estimated 27 million people in Europe and North America and is characterized by the formation of atherosclerotic plaques that limit blood flow to the legs [1,2]. The primary manifestation of PAD is claudication, a severe functional limitation identified as walking-induced pain or cramping in the muscles of the leg, relieved by rest [3]. More advanced disease is characterized by pain while at rest, classified as Fontaine stage III, and nonhealing foot ulcers and gangrene, classified as Fontaine stage IV [3].

Although the primary problem in PAD patients is the presence of atherosclerotic blockages in the arteries supplying their legs [4e7], altered, arterial hemodynamics is not the only cause of functional limitation in the lower limbs of PAD patients [8e14]. Several laboratories have demonstrated that a myopathy is present in the legs of patients with PAD and is a key component of the pathophysiology of PAD [4e6]. A number of studies based on light and electron microscopic evaluation of skeletal muscle from the legs of PAD patients have demonstrated that this myopathy is characterized by substantial abnormalities of the PAD muscle as illustrated in Figures 1 and 2. These abnormalities include myofiber degeneration with alteration of the size and shape of the myofibers, internal nuclei, target lesions, vacuolization, shift of myofiber phenotype toward type I fibers, myofiber necrosis, fatty infiltration, and endomysial and perimysial fibrosis [15e19]. Our group has quantified, precisely, parameters of myofiber morphology in PAD and control gastrocnemius samples obtained with minimally invasive needle biopsy. We found consistent and quantifiable changes in gastrocnemius myofiber morphology, which can separate PAD patients from controls and PAD patients with stage II disease from patients with critical limb ischemia [18,20]. In the present study, we evaluated myofiber morphometrics as predictors of objective measures of the limb function (calf muscle strength and walking distances) of PAD patients. We hypothesized that in PAD patients, morphometric parameters of gastrocnemius myofibers correlate with calf muscle strength and walking distances.

2. Material and methods

2.1. Human subjects

The experimental protocol was approved by the Institutional Review Board, of the VA Nebraska-Western Iowa and the University of Nebraska Medical Centers, and all subjects gave informed consent. We recruited 154 patients evaluated for symptomatic PAD. For every patient, the diagnosis of PAD was established on the basis of medical

history, physical examination, significantly decreased ankle-brachial index (ABI), and computerized or standard arteriography. We specifically excluded patients that had exercise capacity limited by conditions other than claudication including leg (joint/musculo-skeletal, neurologic) and systemic (heart, lung disease) pathology. We recruited 85 patients with normal blood flow to their lower limbs, undergoing lower extremity operations for indications other than PAD. These patients had no history of PAD symptoms, and all had normal lower extremity pulses at examination. All controls were selected to have normal ABIs at rest and after stress and all led sedentary lifestyles.

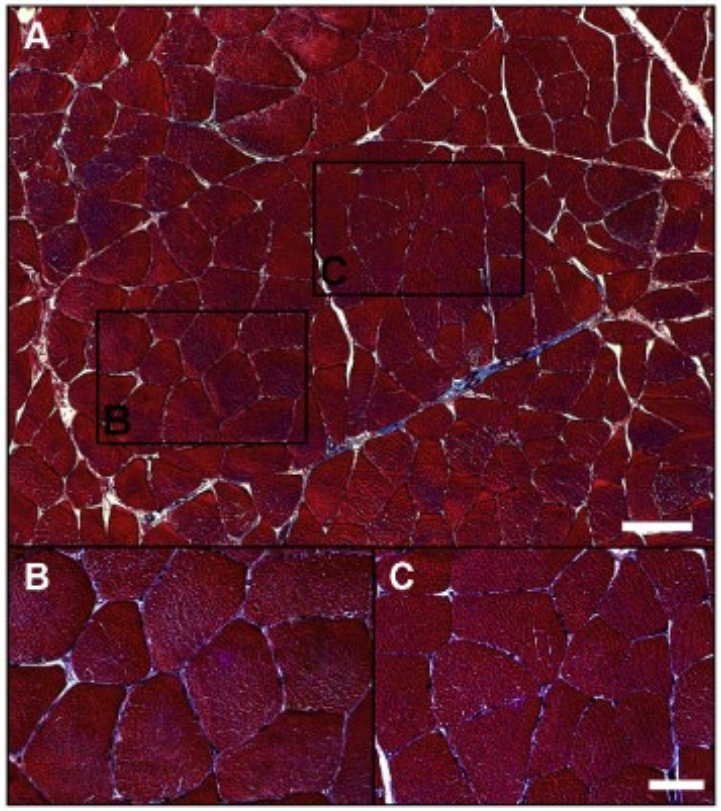

Fig. 1 – Normal histology of the gastrocnemius of a control patient. The muscle biopsy was fixed in methacarn, embedded in paraffin, and sectioned at 4 μm. Slide-mounted sections were stained with Masson trichrome and captured with a ×10 objective (panel A). Regions identified with black frames were captured with a ×40 objective and are presented as separate panels (B and C). The myofibers (red), exhibiting a regular polygonal shape, little size variation, and peripherally located nuclei (black), were tightly packed within a thin investment of connective tissue (blue). The white bars represent 100 μm (panel A) and 50 μm (panels B and C). (Color version of figure is available online.)

2.2. Muscle biopsy

Gastrocnemius samples were obtained from the anteromedial aspect of the muscle belly, 10-cm distal to the tibial tuberosity. All biopsies were obtained with a 6-mm Bergstrom needle. The samples were placed immediately into cold methacarn. After 48 h in methacarn, the specimens were transferred to cold ethanol:H2O (50:50 v/v) and subsequently embedded in paraffin.

2.3. Histology

Masson trichrome staining was implemented with a kit from Thermo Fisher Scientific (#87019; Waltham, MA) according to the instructions provided with the kit. Briefly, paraffin-embedded biopsy specimens sectioned at 4 mm were deparaffinized and fixed in Bouin solution overnight. After incubation in Weigert iron hematoxylin solution, the slideswere stained with Biebrich scarlet-acid fuchsin and aniline blue and dehydrated in ethanol and xylene. Extensive washes were done between each staining. The collagen was stained blue, the nuclei were stained black, and the myofibers were stained red.

2.4. Fluorescence microscopy

Paraffin-embedded biopsies sectioned at 4 mm were deparaffinized with xylene and rehydrated via a series of ethanol washes and distilled water. The rehydrated slide specimens were heated at 95 C in 100 mM citrate buffer (pH 6.0) for 15 min and then allowed to cool for 20 min. Subsequently, the slide specimens were soaked in Super-Sensitive Wash buffer (SS; BioGenex Laboratories, Freemont, CA) for 30 min at room temperature.

A programmable autostainer (BioGenex i6000; BioGenex Laboratories) was used to label sarcolemma and myosin heavy chains. For labeling of myofibers, specimens were blocked with 10% goat serum and were treated with a mixture of mouse anti-type I myosin heavy chain (M8421, clone NOQ7.5.4D; SigmaeAldrich, St. Louis, MO) and mouse anti-type II myosin heavy chain (M4276, clone MY-32; SigmaeAldrich) antibodies, for 1 h. Subsequently, the slides were treated for 1 h with a mixture of goat anti-mouse IgG-Alexa Fluor 488 (A11029, Molecular Probes; Life Technologies, Grand Island, NY) and wheat germ agglutinin-Alexa Fluor 647, which label sarcolemma (W32466, Molecular Probes; Life Technologies). Finally, Pro-Long Gold antifade medium with the nuclear label 40,6-dia-midino-2-phenylindole (P36931, Molecular Probes; Life Technologies) was applied to the labeled specimens.

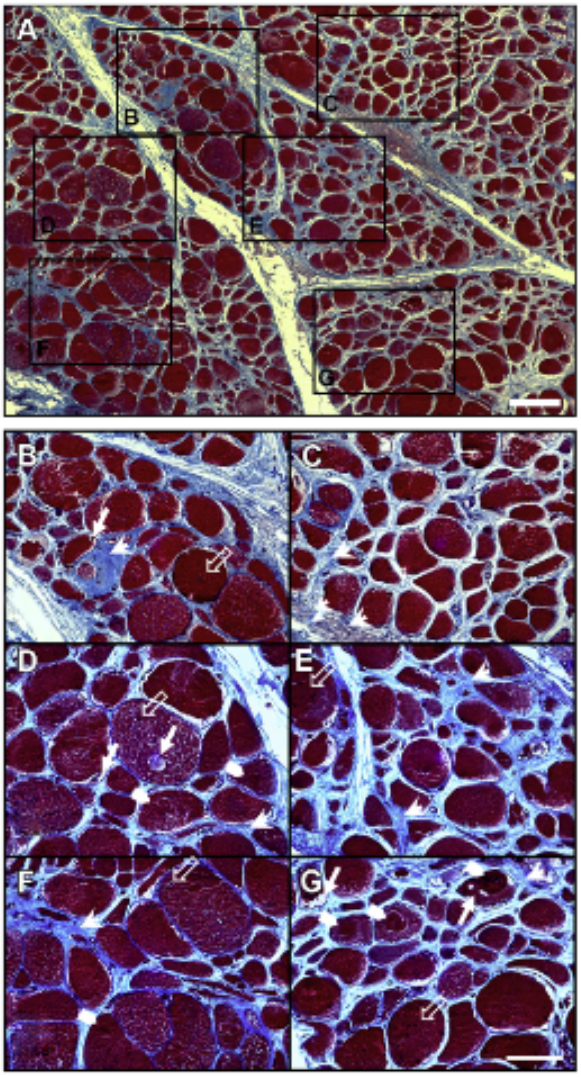

Fig. 2 — Severe myopathy in the gastrocnemius of a patient with PAD. The muscle biopsy was fixed in methacarn, embedded in paraffin, and sectioned at 4 μm. Slide-mounted sections were stained with Masson trichrome and captured with a ×10 objective (panel A). The myofibers (red), exhibiting a nonpolygonal round shape, large variation in size and nuclei (black) often present in the interior, were embedded in an abundant collagenous matrix (blue). Regions identified with black frames were captured with a ×40 objective and are presented as separate panels (B—G; next page). Degradation and loss of myofibers, clearly apparent in panels (B—G), are associated with a remarkable increase of collagen deposition (arrow heads) in the extracellular matrix and the appearance of myofiber vacuoles (filled arrows), target lesions (chevrons), and more centrally located nuclei (unfilled arrows). The white bars represent 100 μm (panel A) and 50 μm (Panels B—G). (Color version of figure is available online.)

2.5. Image acquisition and analysis

Gray-scale (12-bit) fluorescence images (1344 x 1044) were captured with a wide-field, epifluorescence microscope (Leica DMRXA2; North Central Instruments, Plymouth, MN) (x10 objective; 0.5128 mm/pixel), a B/W CCD camera (Orca ER C4742-95; Hamamatsu Photonics, Bridgewater, NJ), and HCImage Hamamatsu software (64-bit version 4.2.5; Hamamatsu Photonics). An acquisition matrix was programmed into the HCImage software to cover the whole muscle specimen area, acquiring 100e150 microscopic frames per specimen yielding images of 134,400 x 104,400 to 201,600 x 156,600 pixels. At each location, images were collected in fluorescence channels corresponding to each fluorophore; 1) 40,6-diamidino-2-phenylindole (nuclei) with an excitation maximum at 358 nm and emission maximum at 461 nm, 2) Alexa Fluor 488 (myosin heavy chains) with an excitation maximum at 495 nm and emission maximum at 519 nm, and 3) Alexa Fluor 647 (sarcolemma) with an excitation maximum 650 nm and emission maximum at 668 nm. The frames corresponding to each fluorophore were montaged in one large image to represent the given (whole) specimen. Image segmentation was done with a custom-made Matlab algorithm (R2012a; MathWorks Inc, Natick, MA), using thresholding, edge detection, regionprops, and a set of heuristics [18,20]. Labeled sarcolemma acquired at 668 nm provided a binary image that served as an outline for each myofiber. The sarcolemma outline was then super-imposed on the image of myosin heavy chains, allowing precise identification of the myofibers for analysis. For each specimen, we extracted measurements of myofiber size, shape, and density. The methods describing how these parameters were measured have been described in detail [18,20]. Briefly, we calculated the following parameters of myofiber size: 1) myofiber cross-sectional area (μ^2), from the number of pixels enclosed within a segmented myofiber, 2) major and minor axes (μ), of an ellipse fitted in the myofiber, 3) equivalent diameter (μ), as the diameter of a circle that has the same area as the segmented myofiber, and 4) myofiber perimeter (μ), from the number of pixels on the boundary of the myofiber. We calculated the following parameters of myofiber shape: 1) roundness, as the equivalent diameter x π divided by the perimeter of the segmented myofiber, and 2) solidity, defined as the myofiber cross-sectional area divided by the area of a fitted convex hull. A fitted convex hull is the smallest convex polygon that can encompass the myofiber. Finally, myofiber density was measured as the area occupied by the myofibers divided by the area occupied by the myofibers plus interstitial tissue. In terms of biological relevance, we expect that these mathematical equations will provide objective measures that quantitatively reflect pathologic changes in the muscle, including myofiber degeneration, necrosis, or apoptosis (myofiber cross-sectional area, perimeter, equivalent diameter, roundness, and solidity), loss of the normal polygonal myofiber shape (myofiber roundness and solidity), and replacement of muscle by fibrous and/or adipose tissues (myofiber density).

2.6. Muscle strength measurement

Muscle force production from the ankle plantar flexors was measured using a Biodex dynamometer (System 4.0; Biodex Medical Systems, Shirley, NY). The PAD patients were secured onto the Biodex and the standard ankle plantar

flexion/dorsiflexion position of 90 angle between the foot and the shank was used. To isolate the plantar flexor muscles, the ipsilateral thigh, waist, and chest of the patients were secured. The parameter of the muscle strength we measured was the peak force produced by the ankle plantar flexors (the muscles of the posterior compartments of the calf) during a maximum isometric contraction of 10-s duration. Data are represented in ft x lbs.

2.7. Graded treadmill test and 6-min walking distance

Maximum walking distance was measured for all PAD patients using the Gardner graded treadmill test. The patients walked at a constant speed of 3.2 $km \cdot h^{-1}$ on a 0º grade, followed by 2º grade increase every 2 min. All PAD patients were also evaluated with the 6-min walk test. The test was performed in an indoor 20-m hallway for 6 min. The procedure was performed under technical supervision, and the patient was given instructions to cover as much distance as possible.

2.8. Statistical analyses

Baseline characteristics between PAD patients and control subjects were compared using chi-square or Fisher exact tests for categorical variables and independent t-tests for continuous variables. A one-way analysis of covariance was used to identify differences between PAD and control groups for all the morphometric parameters adjusting for any significant covariates. Bivariate correlations were used to correlate morphometric parameters with limb function and muscle strength parameters. The data were standardized, and multiple regression analyses with stepwise regression were used to identify predictors of calf muscle strength and walking distances. All analyses were performed using SAS statistical software version 9.3 (SAS Institute Inc, Cary, NC). All the data are presented as mean standard error of the mean.

3. Results

3.1. Subject demographics

The demographic information for both the PAD and control subjects is presented in Table 1. Gender (χ^2 = 18.8, P < 0.001), smoking status (χ^2 = 25.3, P < 0.001), coronary artery disease (χ^2 = 5.4, P = 0.022), family history of PAD (χ^2 = 4.6, P = 0.036), dyslipidemia (χ^2 = 5.3, P =0.029) and ABI (t =

20.3, P < 0.001) were significantly different between the PAD and control subjects. Subsequently, these parameters were used as covariates in the rest of the analyses to control their effects on the myopathy of PAD.

3.2. Gastrocnemius specimens of PAD patients exhibited abnormal myofiber morphology and density compared with controls

In PAD gastrocnemius, myofiber cross-sectional area, major axis, minor axis, equivalent diameter, and perimeter, were significantly reduced compared with those of controls. Moreover, PAD myofibers exhibited abnormal shape having increased roundness and decreased solidity. Finally, we observed a decrease in myofiber density per unit area of cross-sectioned specimen (Table 2).

Table 1 – Baseline characteristics of control and PAD patients.

Baseline characteristics	Control	PAD	*P* value
Number of subjects	85	154	N/A
Mean age (y)	62.5 ± 9.8	62.9 ± 7.5	0.738
Height (m)	1.76 ± 0.08	1.76 ± 0.07	0.959
Weight (kg)	91.2 ± 16.9	86.67 ± 18.4	0.066
ABI	1.08 ± 0.08	0.51 ± 0.25	<0.001
RACE % (W/AA/H/IND)	95.2/2.4/ 2.4/0	91.6/7.1/ 0.65/0.65	0.240
Gender % (male/female)	81.2/18.8	97.4/2.6	<0.001
Smoking status % (never/ current/former)	42.4/30.5/ 27.1	3.9/60.4/ 35.7	<0.001
Coronary artery disease, %	23.50	38.30	0.022
Family history of PAD, %	20.00	33.10	0.036
Obesity, %	31.80	25.30	0.294
Diabetes, %	23.50	31.80	0.184
Dyslipidemia, %	58.80	73.40	0.029
Hypertension, %	67.10	77.90	0.089

N/A = not applicable.
Race, (W) White, (AA) African American, (H) Hispanic, (IND) American Indian.

Table 2 – Myofiber morphometrics of the gastrocnemius of control and PAD patients.

Myofiber morphometrics	Control	PAD	*P* value
Cross-sectional area (μ^2)	5047 ± 139	4215 ± 100	<0.001
Major axis (μ)	104.48 ± 2.1	96.53 ± 1.5	0.003
Minor axis (μ)	60.06 ± 1.7	53.51 ± 1.3	0.003
Equivalent diameter (μ)	76.21 ± 1.2	70.64 ± 0.8	<0.001
Perimeter (μ)	303.79 ± 5.6	280.57 ± 4.1	0.001
Roundness	0.799 ± 0.004	0.814 ± 0.003	0.005
Solidity	0.947 ± 0.002	0.938 ± 0.001	<0.001
Myofiber density	0.823 ± 0.007	0.772 ± 0.005	<0.001

P values were adjusted for ABI, dyslipidemia, coronary artery disease, gender, and family history of PAD.

3.3. Calf muscle strength and walking distances of PAD patients change with myofiber morphology and density

The observed differences between PAD and control gastrocnemius myofibers suggested that myofiber morphometrics may correlate with calf muscle strength and walking distances (Table 3). Calf muscle strength increased with increasing myofiber cross-sectional area, major axis, minor axis, equivalent diameter, perimeter, solidity, and fiber density. In contrast, calf muscle strength decreased with increasing myofiber roundness, a measure of abnormal myofiber morphology. Similarly, 6-min walking distance increased with increasing myofiber cross-sectional area, major axis, equivalent diameter, perimeter, solidity, and fiber density and decreased with increasing myofiber roundness. Finally, maximum walking distance increased with increasing myofiber cross-sectional area, major axis, minor axis, and equivalent diameter and perimeter increased with increasing maximum walking distance and decreased with increasing myofiber roundness. Based on these observations, we performed multiple regression analyses with stepwise regression to identify the best morphometric predictors of calf muscle strength and walking distances. Calf muscle strength was predicted by myofiber cross-sectional area, roundness, and solidity (r^2 = 0.617, r = 0.786, P < 0.001) according to the following equation:

Calf Muscle Strength (ft * lbs) = 123 + 0.450 * *Area* – 0.333

Roundness + 0:260 * *Solidity*

Table 3 – Correlations of myofiber morphometrics in the PAD gastrocnemius with calf muscle strength and walking distances.

Myofiber morphometrics	Calf muscle strength (ft × lbs)	6 min walking distance (m)	Maximum walking distance (m)
ABI	0.401†	0.217*	0.211*
Cross-sectional area (μ²)	0.615†	0.443†	0.483†
Major axis (μ)	0.608†	0.360†	0.390†
Minor axis (μ)	0.419†	0.103	0.201*
Equivalent diameter (μ)	0.587†	0.391†	0.408†
Perimeter (μ)	0.60†	0.382†	0.342†
Roundness	−0.430†	−0.285*	−0.204*
Solidity	0.486†	0.251*	0.105
Myofiber density	0.219*	0.221*	0.125

*P < 0.05.
†P < 0.001.

Plots of calf muscle strength versus myofiber cross-sectional area, roundness, and solidity are presented in Figure 3. Six-minute walking distance was predicted by myofiber cross-sectional area, roundness, and solidity (r^2 – 0.321, r – 0.566, P < 0.001) according to the following equation:

$$\textit{Six Minute Walking Distance}\ (m) = -586 + 0{:}388 * \textit{Area} - 0{:}180 * \text{Roundness} + 0{:}179 * \text{Solidity}$$

Maximum walking distance was predicted only by myofiber cross-sectional area (r^2 = 0.295, r – 0.543, P < 0.001) according to the following equation:

$$\textit{Maximum Walking Distance}\ (m) - -107 + 0{:}543 * \textit{Area}$$

4. Discussion

Our study shows that precise morphometric analysis of needle biopsy specimens identifies specific and consistent aberrations in the gastrocnemius myofibers of patients with PAD. More importantly, our data show, for the first time, that these objectively defined parameters of gastrocnemius myofiber morphology are closely linked to the calf muscle strength and walking distances of claudicating PAD patients. Using fluorescence microscopy and detailed image processing, we demonstrated that multiple parameters of myofiber size (cross-sectional area, major and minor axes, equivalent diameter, and perimeter), shape (roundness and solidity), and density are significantly altered in the PAD gastrocnemius compared with those of control. Furthermore, using statistical modeling, we found that the changes in the cross-sectional area, roundness, and solidity of the gastrocnemius myofibers are strong predictors of muscle strength and 6-min and maximum walking distances of the claudicating patients.

Our report represents, thus far, the largest quantitative study of the histopathology of the affected skeletal muscle of claudicating patients. A widely held view concerning the pathophysiology of claudication has been that limb dysfunction and walking limitation of claudicating patients are produced exclusively by exercise-induced ischemia in the muscles of the lower limb. Published work from our group and others [4-6,21] has revised this view by documenting the presence of a myopathy in leg muscles of patients with PAD and demonstrating a constellation of baseline, gait abnormalities of rested patients, before the onset of claudication [10,11,22e25], when tissue oxygen levels [26] and blood flow [13] in the leg are similar to (and sometimes even higher than) those of controls. Furthermore, measurements of muscle strength in PAD patients determined as 5-s maximal isometric strength, a blood flow-independent assessment [12], demonstrated that muscle strength in PAD patients is significantly reduced compared with that of controls. The present work lends particular support to the importance of myopathy to the functional impairment of patients with claudication by establishing the presence of a strong correlation between myofiber morphometrics and both calf muscle strength and walking distances. Our data demonstrate that myofiber

morphometric parameters (including combinations of cross-sectional area, major axis, minor axis, equivalent diameter, perimeter, roundness, solidity, and density) were stronger correlates of calf muscle strength, 6-min walking distance and treadmill maximum walking distance than ABI, which represents the degree of arterial obstruction.

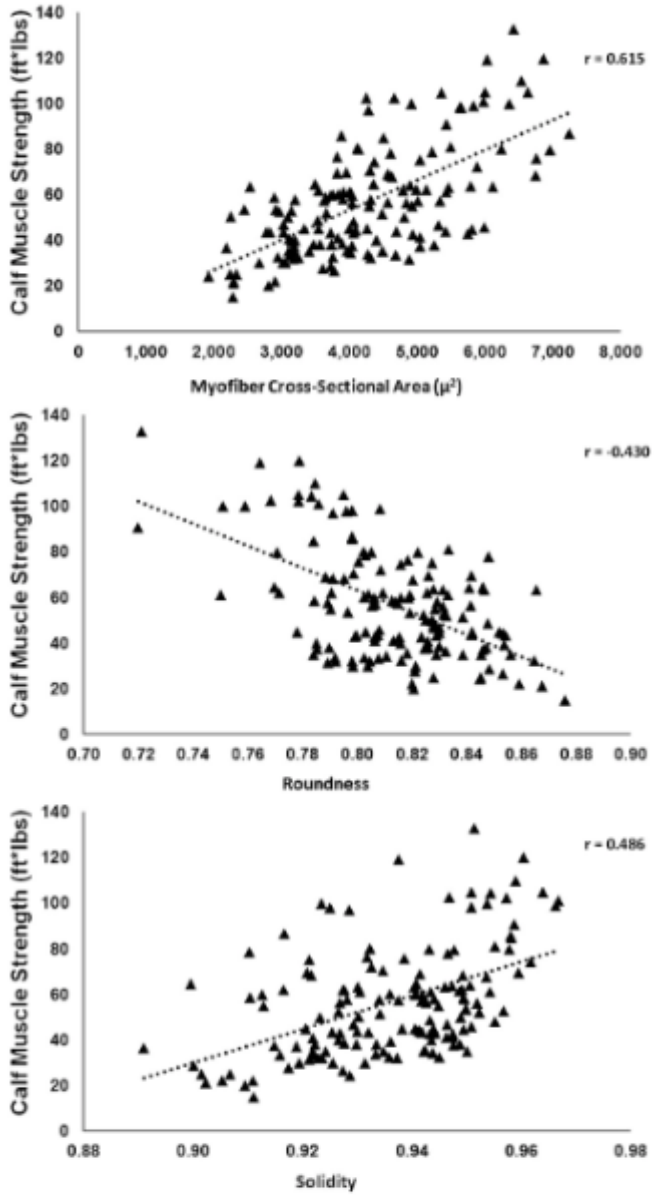

Fig. 3 – Scatterplots showing correlations between calf muscle strength and myofiber cross-sectional area (μ^2), roundness, and solidity in claudicating patients ($n = 154$). Calf muscle strength increased with increasing myofiber cross-sectional area and solidity and decreased with increasing myofiber roundness.

The myopathy of claudicating muscle is readily observed in histologic preparations of gastrocnemius specimens from PAD patients (Figs. 1 and 2). PAD muscle displays different patterns of myofiber degeneration with alteration of the size and shape of the myofibers [2,15,18,19], internal nuclei, target lesions, vacuolization, shift of myofiber phenotype toward type I fibers, myofiber necrosis, fatty infiltration and endomysial, perimysial and epimysial fibrosis [15-19]. In addition, the myopathy of PAD muscle has been observed by computerized tomographic scanning of the calf muscles of claudicating patients, demonstrating smaller muscle volume, higher fat content, and lower muscle density [27]. More detailed evaluation of the ultrastructure, physiology, and biochemistry of claudicating muscle reveals that the primary pathophysiological features of this myopathy are mitochondrial dysfunction, oxidative damage, and inflammation [2,6,27-30]. The widely held view is that PAD myopathy is caused by repetitive cycles of ischemiaereperfusion [4e6], which initiate mitochondrial dysfunction and injury and produce inflammation and oxidative damage. In the long term, repeated oxidative and inflammatory insults to the myofiber [31-33] are expected to produce myofiber degeneration and the associated changes in the myofiber morphometry we have established with our present work.

This is a correlational study demonstrating that the myofiber size and shape are abnormal in PAD gastrocnemius and that these changes correlate with limb dysfunction (impaired calf muscle strength and walking distances) in PAD patients. The study does not identify cause/effect relationships; however, the high quality human data we have produced demonstrate that grading of myofiber degeneration can serve as a measure of the progression of damage and dysfunction in PAD limbs and may allow objective determination, at the tissue level, of the outcomes produced by pharmacologic and surgical therapies in patients with PAD.

The association between myofiber characteristics and limb function has been observed in a small number of studies of patients with pathologic states that affect the skeletal muscles of the lower extremities and healthy volunteers. In a study of 10 patients with unilateral PAD [19], gastrocnemius muscle strength of the symptomatic leg correlated with total calf cross-sectional area and cross-sectional area occupied by type II myofibers. The study did not have enough power to explore correlations with maximum walking time or area occupied by type I myofibers. In a slightly larger study of 25 males with limb-girdle muscular dystrophy 2A [34], myofiber size correlated with the clinical disability score of the patients [34]. Expression of muscle-specific RING finger protein 1, a ubiquitin-protein ligase closely associated with myofiber proteolysis, was increased in limb-girdle muscular dystrophy 2A muscle and correlated with reduced myofiber cross-sectional area and decreased muscle performance. Finally, in a study of the quadriceps muscle of 48 college students [35], immobilization reduced myosin heavy chain transcripts in association with reduced myofiber cross-sectional area and reduced muscle strength. After retraining, muscle fiber cross-sectional increased in association with increased muscle strength. It will be of interest to evaluate the effects of interventions including exercise therapy, nutritional therapy, and pharmacotherapy

with medications that enhance mitochondrial function and antioxidant defenses, androgens, growth hormone, ghrelin, myostatin inhibitors, and anti-inflammatory agents [36-40] on myofiber morphometrics in relation to muscle strength and leg function of patients with PAD.

5. Conclusions

In summary, morphologic damage to myofibers can be precisely quantified using gastrocnemius specimens obtained with minimally invasive needle biopsy. Statistical modeling based on myofiber morphometrics established a correlation between advancing myofiber degeneration and functional decline in PAD patients. Our work has established a comprehensive profile of quantitative morphometric changes in PAD muscle, which can serve as a guide for more extensive mechanisms and intervention studies essential for much needed improvement of diagnosis, staging, and treatment of PAD.

Acknowledgment

This work was primarily supported by NIH grant R01AG034995, by the Charles and Mary Heider Fund for Excellence in Vascular Surgery, by the Alexander S. Onassis Public Benefit Foundation F-ZD036, and by the American Heart Association Pre-Doctoral Fellowship 13PRE13860010. Secondary funding was provided by the Department of Veterans' Affairs, Veterans Health Administration, Rehabilitation Research, and Development Service 1I01RX000604 and by the National Institute of General Medical Sciences of the National Institutes of Health under Award Number P20GM109090. The content of this paper is solely the responsibility of the authors and does not necessarily represent the official views of the National Institutes of Health. Furthermore, this material is the result of work supported with resources and the use of facilities at the VA Nebraska-Western Iowa Health Care System.

Authorship note: G.P.C. and I.I.P. are co-senior authors.

Authors' contributions: P.K., G.P.C., and I.I.P. contributed to the conception and design. P.K., S.A.M., K.C., D.M., E.P., G.H., R.D.M., and G.P.C. analyzed the experimental data. P.K., J.M.J., D.M., E.P., and I.I.P. collected muscle specimens. P.K., S.A.M., D.M., K.C., E.P., D.M.H., K.U., and I.I.P. collected and analyzed clinical data. G.H. and P.K. performed the statistical analysis. P.K., G.H., R.D.M., S.A.M., K.U., G.P.C., and I.I.P. drafted and made critical revisions to the article.

Disclosure

The authors reported no proprietary or commercial interest in any product mentioned or concept discussed in the article.

REFERENCES

[1] Roger VL, Go AS, Lloyd-Jones DM, et al. American Heart Association Statistics C. Stroke Statistics Subcommittee. Executive summary: heart disease and stroke statisticsd2012 update: a report from the American Heart Association. Circulation 2012;125:188.

[2] Weiss DJ, Casale GP, Koutakis P, et al. Oxidative damage and myofiber degeneration in the gastrocnemius of patients with peripheral arterial disease. J Translational Med 2013;11:230.

[3] Norgren L, Hiatt WR, Dormandy JA, et al. Inter-society consensus for the management of peripheral arterial disease (TASC II). J Vasc Surg 2007;45(Suppl S):S5.

[4] Brass EP, Hiatt WR. Acquired skeletal muscle metabolic myopathy in atherosclerotic peripheral arterial disease. Vasc Med 2000;5:55.

[5] Pipinos II, Judge AR, Selsby JT, et al. The myopathy of peripheral arterial occlusive disease: part 1. Functional and histomorphological changes and evidence for mitochondrial dysfunction. Vasc Endovascular Surg 2007;41:481.

[6] Pipinos II, Judge AR, Selsby JT, et al. The myopathy of peripheral arterial occlusive disease: part 2. Oxidative stress, neuropathy, and shift in muscle fiber type. Vasc Endovascular Surg 2008;42:101.

[7] McDermott MM, Liu K, Tian L, et al. Calf muscle characteristics, strength measures, and mortality in peripheral arterial disease: a longitudinal study. J Am Coll Cardiol 2012;59:1159.

[8] Gardner AW, Killewich LA. Lack of functional benefits following infrainguinal bypass in peripheral arterial occlusive disease patients. Vasc Med 2001;6:9.

[9] Gardner AW, Skinner JS, Cantwell BW, Smith LK. Prediction of claudication pain from clinical measurements obtained at rest. Med Sci Sports Exerc 1992;24:163.

[10] Koutakis P, Johanning JM, Haynatzki GR, et al. Abnormal joint powers before and after the onset of claudication symptoms. J Vasc Surg 2010;52:340.

[11] Koutakis P, Pipinos II, Myers SA, Stergiou N, Lynch TG, Johanning JM. Joint torques and powers are reduced during ambulation for both limbs in patients with unilateral claudication. J Vasc Surg 2010;51:80.

[12] McDermott MM, Criqui MH, Greenland P, et al. Leg strength in peripheral arterial disease: associations with disease severity and lower-extremity performance. J Vasc Surg 2004; 39:523.

[13] Pernow B, Zetterquist S. Metabolic evaluation of the leg blood flow in claudicating patients with arterial obstructions at different levels. Scand J Clin Lab Invest 1968;21:277.

[14] Pipinos II, Judge AR, Zhu Z, et al. Mitochondrial defects and oxidative damage in patients with peripheral arterial disease. Free Radic Biol Med 2006;41:262.

[15] Hedberg B, Angquist KA, Henriksson-Larsen K, Sjostrom M. Fibre loss and distribution in skeletal muscle from patients with severe peripheral arterial insufficiency. Eur J Vasc Surg 1989;3:315.

[16] Hedberg B, Angquist KA, Sjostrom M. Peripheral arterial insufficiency and the fine structure of the gastrocnemius muscle. Int Angiol 1988;7:50.

[17] Makitie J, Teravainen H. Histochemical changes in striated muscle in patients with intermittent claudication. Arch Pathol Lab Med 1977;101:658.

[18] Koutakis P, Weiss DJ, Miserlis D, et al. Oxidative damage in the gastrocnemius of patients with peripheral artery disease is myofiber type selective. Redox Biol 2014;2:921.
[19] Regensteiner JG, Wolfel EE, Brass EP, et al. Chronic changes in skeletal muscle histology and function in peripheral arterial disease. Circulation 1993;87:413.
[20] Cluff K, Miserlis D, Naganathan GK, et al. Morphometric analysis of gastrocnemius muscle biopsies from patients with peripheral arterial disease: objective grading of muscle degeneration. Am J Physiol Regul Integr Comp Physiol 2013; 305:R291.
21] Koutakis P, Miserlis D, Myers SA, et al. Abnormal accumulation of desmin in gastrocnemius myofibers of patients with peripheral artery disease: associations with altered myofiber morphology and density, mitochondrial dysfunction and impaired limb function. J Histochem Cytochem 2015;63:256.
[22] Celis R, Pipinos II, Scott-Pandorf MM, Myers SA, Stergiou N, Johanning JM. Peripheral arterial disease affects kinematics during walking. J Vasc Surg 2009;49:127.
[23] Myers SA, Pipinos II, Johanning JM, Stergiou N. Gait variability of patients with intermittent claudication is similar before and after the onset of claudication pain. Clin Biomech 2011;26:729.
[24] Scott-Pandorf MM, Stergiou N, Johanning JM, Robinson L, Lynch TG, Pipinos II. Peripheral arterial disease affects ground reaction forces during walking. J Vasc Surg 2007;46:491.
[25] Wurdeman SR, Koutakis P, Myers SA, Johanning JM, Pipinos II, Stergiou N. Patients with peripheral arterial disease exhibit reduced joint powers compared to velocity-matched controls. Gait & Posture 2012;36:506.
[26] Bauer TA, Brass EP, Hiatt WR. Impaired muscle oxygen use at onset of exercise in peripheral arterial disease. J Vasc Surg 2004;40:488.
[27] McDermott MM, Guralnik JM, Ferrucci L, et al. Physical activity, walking exercise, and calf skeletal muscle characteristics in patients with peripheral arterial disease. J Vasc Surg 2007;46:87.
[28] Makris KI, Nella AA, Zhu Z, et al. Mitochondriopathy of peripheral arterial disease. Vascular 2007;15:336.
[29] Brevetti G, Giugliano G, Brevetti L, Hiatt WR. Inflammation in peripheral artery disease. Circulation 2010;122:1862.
[30] Spirig R, Tsui J, Shaw S. The emerging role of TLR and innate immunity in cardiovascular disease. Cardiol Res Pract 2012; 2012:181394.
[31] Bloch RJ, Gonzalez-Serratos H. Lateral force transmission across costameres in skeletal muscle. Exerc Sport Sci Rev 2003;31:73.
[32] Sanger JW, Sanger JM, Franzini-Armstrong C. Assembly of the skeletal muscle cell. In: Engel AG, Franzini-Armstrong C, editors. Myology. New York, NY, USA: McGraw-Hill; 2004. p. 45.
[33] Sanger JW, Wang J, Fan Y, White J, Sanger JM. Assembly and dynamics of myofibrils. J Biomed Biotechnol 2010;2010: 858606.
[34] Fanin M, Nascimbeni AC, Angelini C. Muscle atrophy in limb girdle muscular dystrophy 2A: a morphometric and molecular study. Neuropathol Appl Neurobiol 2013;39: 762.

[35] Hortobagyi T, Dempsey L, Fraser D, et al. Changes in muscle strength, muscle fibre size and myofibrillar gene expression after immobilization and retraining in humans. J Physiol 2000;524(Pt 1):293.
[36] Dodson S, Baracos VE, Jatoi A, et al. Muscle wasting in cancer cachexia: clinical implications, diagnosis, and emerging treatment strategies. Annu Rev Med 2011;62:265.
[37] Creasy TS, McMillan PJ, Fletcher EW, Collin J, Morris PJ. Is percutaneous transluminal angioplasty better than exercise for claudication? Preliminary results from a prospective randomised trial. Eur J Vasc Surg 1990;4:135.
[38] Brotto M, Abreu EL. Sarcopenia: pharmacology of today and tomorrow. J Pharmacol Exp Ther 2012;343:540.
[39] Barillaro C, Liperoti R, Martone AM, Onder G, Landi F. The new metabolic treatments for sarcopenia. Aging Clin Exp Res 2013;25:119.
[40] Chumlea WC, Cesari M, Evans WJ, et al. International Working Group on Sarcopenia Task Force Members. Sarcopenia: designing phase IIB trials. J Nutr Health Aging 2011;15:450.